The degenerate Payne rearrangement of the 2,3-epoxypropoxide anion in the gas phase. A joint theoretical and experimental study

Suresh Dua, Mark S. Taylor, Mark A. Buntine and John H. Bowie

Department of Chemistry, The University of Adelaide, South Australia, 5005

***Ab initio* calculations [at G2 level] indicate that an energised 2,3-epoxypropoxide anion should undergo two competing cyclisation processes, *i.e.* (*i*) the degenerate Payne rearrangement (attack of O^- at the more substituted carbon of the ethylene oxide ring, to open that ring, and to form another ethylene oxide ring) (the computed barrier to the transition state is 45 kJ mol^{-1}), and (*ii*) attack of O^- at the less substituted carbon of the ethylene oxide ring. This cyclisation forms a more stable oxetane species, but the barrier (from the reactant to transition state) is 122 kJ mol^{-1}. Experimental results are in accord with this prediction. The major fragmentation of energised 2,3-epoxypropoxide is loss of CH_2O to yield a product anion identified as the acetaldehyde enolate anion $(CH_2CHO)^-$. This cleavage can be used as a probe to investigate the relative extents of the two possible cyclisation processes. Comparison of the spectra of the 2,3-epoxypropoxide anion and the $(M - H)^-$ ion from 3-hydroxyoxetane, together with studies of labelled (^2H), and doubly labelled (^2H, ^{18}O) analogues, demonstrate (*a*) that 40% of CH_2O loss occurs by simple cleavage before any rearrangement of the 2,3-epoxypropoxide anion , (*b*) 25% of CH_2O loss follows Payne equilibration, and (*iii*) 35% of CH_2O loss occurs following equilibration of the Payne product and an oxetane intermediate.**

Introduction

The prototypical Payne rearrangement is shown in Scheme 1.

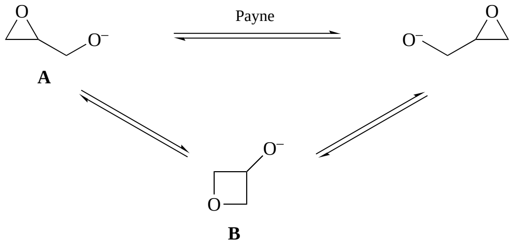

Scheme 1

The rearrangement involves cyclisation of the alkoxide centre at the more substituted carbon of the epoxide ring to open the initial three-membered ring and form a new one. In solution, the reaction is normally carried out at reflux in aqueous sodium hydroxide (or using sodium hydroxide in a mixture of water and a suitable alcohol).[1] The Payne rearrangement shown in Scheme 1 has not been reported, but similar rearrangements of alkyl substituted 2,3-epoxypropoxide anions involve equilibria with the more abundant component of the equilibrium mixture having the substituents on the ring rather than on the side chain.[1] There is no evidence to suggest that in solution, the Payne rearrangement co-occurs with cyclisation to form the alternative four-membered oxetane system (see Scheme 1 for the prototypical system **B**). The Payne rearrangement has been shown[2,3] to be of synthetic utility.

We wish to explore, in the gas phase, the scenario summarised in Scheme 1. The gas phase study will establish the fundamental reactivity of system **A**, *i.e.* the reactivity in the absence of any possible solvent or counter ion effects. This paper reports the results of a joint theoretical and experimental study planned to answer the following questions. (*i*) Does the Payne rearrangement occur following collisional activation of the 2,3-epoxypropoxide anion in the gas phase? (*ii*) If the answer to (*i*) is yes, does the formation of oxetane anion **B** (see Scheme 1) compete with the Payne rearrangement?

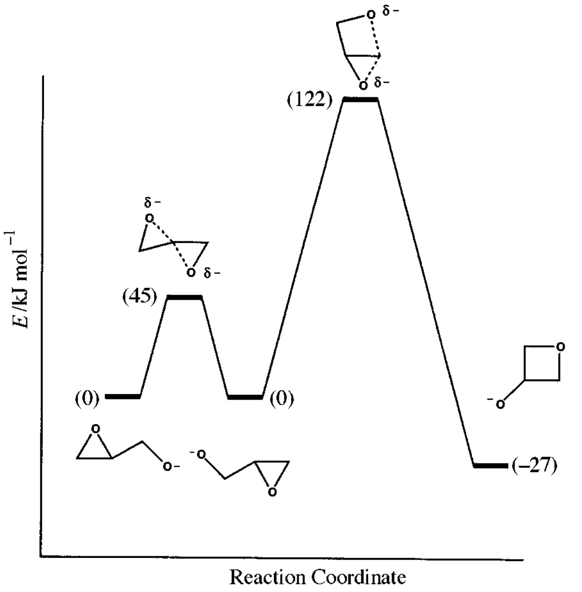

Fig. 1 G2 calculations for the Payne rearrangement and the interconversion of **A** to **B**. See Experimental section for procedural details, and Table 1 for geometries and energies of **A**, **B** and the two transition states.

Results and discussion

The results of an *ab initio* computational study [at G2 level] using GAUSSIAN94[4] are summarised in Fig. 1. Full details of the geometries and energies of **A** and **B**, and of the two transition states are recorded in Table 1. Gas phase reactions are generally kinetically controlled. Rates of reaction are controlled primarily by two factors, *viz.* the barrier to the transition state, and the probability of reaction (frequency factor, the pre-experimental Arrhenius factor)[5] in the rate equation. Reaction coordinate plots of the type shown in Fig. 1 provide primary data concerning the first of these parameters, *i.e.* the barrier to the transition state. The barrier for the degenerate Payne rearrangement shown in Fig. 1 is 45 kJ mol^{-1}: such a small

Table 1 Energies and geometries [bond lengths (Å), bond angles (°) and dihedral angles (°)] of species shown in Fig. 1 [MP2(full)/6-31g(d) optimised]

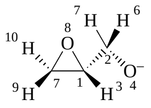

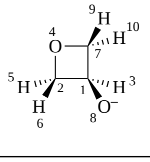

G2 (0 K)		−267.309 354 hartrees (0 kJ mol^{-1})		−267.319 521 hartrees (0 kJ mol^{-1})			
G2 [MP2 (0 K)]		−267.302 108 (−26.69)		−267.312 689 (−27.78)			
C^2C^1	1.530	$O^4C^2C^1H^3$	54.33	C^2C^1	1.587	$O^4C^2C^1H^3$	−84.17
H^3C^1	1.093	$O^4C^2C^1C^7$	−94.20	H^3C^1	1.140	$O^4C^2C^1C^7$	17.40
O^4C^2	1.331	$O^4C^2C^1O^8$	−165.09	O^4C^2	1.453	$O^4C^2C^1O^8$	140.18
H^5C^2	1.140	$H^5C^2C^1H^3$	−72.28	H^5C^2	1.103	$H^5C^2C^1H^3$	162.30
H^6C^2	1.141	$H^5C^2C^1C^7$	139.19	H^6C^2	1.102	$H^5C^2C^1C^7$	−96.13
C^7C^1	1.457	$H^5C^2C^1O^8$	68.29	C^7C^1	1.588	$H^5C^2C^1O^8$	26.65
O^8C^1	1.474	$H^6C^2C^1H^3$	−178.87	C^7O^4	1.453	$H^6C^2C^1H^3$	32.65
O^8C^7	1.442	$H^6C^2C^1C^7$	32.56	O^8C^1	1.304	$H^6C^2C^1C^7$	134.22
H^9C^7	1.093	$H^6C^2C^1O^8$	−38.30	H^9C^7	1.103	$H^6C^2C^1O^8$	−103.0
$H^{10}C^7$	1.091	$O^8C^7C^1C^2$	−110.64	$H^{10}C^7$	1.102	$H^7O^4C^2C^1$	−18.80
$C^2C^1H^3$	113.54	$O^8C^7C^1H^3$	101.82	$C^2C^1H^3$	103.36	$C^7O^4C^2H^5$	93.07
$C^1C^2O^4$	109.84	$H^9C^7C^1C^2$	145.91	$C^1C^2O^4$	92.08	$C^7O^4C^2H^6$	−143.99
$C^1C^2H^5$	104.95	$H^9C^7C^1H^3$	−1.63	$C^1C^2H^5$	109.48	$O^4C^7C^1C^2$	−17.40
$O^4C^2H^5$	117.03	$H^9C^7C^1O^8$	−103.44	$O^4C^2H^5$	111.34	$O^4C^7C^1H^3$	84.17
$H^5C^2H^6$	101.96	$H^{10}C^7C^1C^2$	−5.77	$C^1C^2H^6$	121.53	$O^4C^7C^1O^8$	−140.18
$C^2C^1C^7$	121.95	$H^{10}C^7C^1H^3$	−153.31	$O^4C^2H^6$	111.43	$H^9C^7C^1C^2$	96.13
$H^3C^1C^7$	116.89	$H^{10}C^7C^1O^8$	104.87	$H^5C^2H^6$	109.78	$H^9C^7C^1H^3$	−162.30
$C^2C^1O^8$	121.95	$C^7O^8C^1C^2$	110.65	$C^2C^1C^7$	80.37	$H^9C^7C^1O^8$	−26.66
$H^3C^1O^8$	112.94	$C^7O^8C^1H^3$	−108.57	$H^3C^1C^7$	103.36	$H^{10}C^7C^1C^2$	−134.22
$C^7C^1O^8$	58.95	$C^1O^8C^7H^9$	113.35	$C^2O^4C^7$	89.68	$H^{10}C^7C^1H^3$	−32.65
$C^1C^7O^8$	61.12	$C^1O^8C^7H^{10}$	−109.67	$C^1C^7O^4$	92.08	$H^{10}C^7C^1O^8$	103.00
$C^1O^8C^7$	59.93			$C^2C^1O^8$	122.67	$C^1C^7O^4C^2$	18.79
$C^1C^7H^9$	121.29			$H^3C^1O^8$	117.44	$H^9C^7O^4C^2$	−93.08
$O^8C^7H^9$	115.14			$C^7C^1O^8$	122.66		
$C^1C^7H^{10}$	118.19			$C^1C^7H^9$	109.48		
$O^8C^7H^{10}$	115.23			$O^4C^7H^9$	111.35		
$H^9C^7H^{10}$	114.69			$C^1C^7H^{10}$	121.53		
$C^1C^2H^6$	103.64			$O^4C^7H^{10}$	111.43		
$O^4C^2H^6$	117.87			$H^9C^7H^{10}$	109.78		

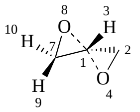

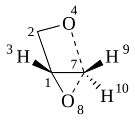

G2 (0 K)		−267.292 031 hartrees (45.48 kJ mol^{-1})		−267.262 896 (121.97)			
G2 [MP2(0 K)]		−267.284 256 (46.87)		−267.255 655 (121.96)			
C^2C^1	1.454	$O^4C^2C^1H^3$	76.27	C^2C^1	1.558	$O^4C^2C^1H^3$	−82.47
H^3C^1	1.080	$O^4C^2C^1C^7$	−103.72	H^3C^1	1.111	$O^4C^2C^1C^7$	35.02
O^4C^2	1.384	$H^5C^2C^1H^3$	−40.70	O^4C^2	1.388	$O^4C^2C^1O^8$	127.51
H^5C^2	1.111	$H^5C^2C^1C^7$	139.30	H^5C^2	1.119	$H^5C^2C^1H^3$	156.78
H^6C^2	1.111	$H^6C^2C^1H^3$	−166.69	H^6C^2	1.111	$H^5C^2C^1C^7$	−85.73
C^7C^1	1.454	$H^6C^2C^1C^7$	13.31	C^7C^1	1.434	$H^5C^2C^1O^8$	6.76
O^8C^7	1.385	$O^8C^7C^1C^2$	−103.72	O^8C^1	1.378	$H^6C^2C^1H^3$	38.49
H^9C^7	1.111	$O^8C^7C^1H^3$	76.28	H^9C^7	1.080	$H^6C^2C^1C^7$	155.98
$C^{10}C^7$	1.111	$H^9C^7C^1C^2$	139.30	$H^{10}C^7$	1.093	$H^6C^2C^1O^8$	−111.53
O^4C^1	1.892	$H^9C^7C^1H^3$	−40.70	O^4C^7	2.082	$H^9C^7C^1C^2$	60.83
O^8C^1	1.892	$H^{10}C^7C^1C^2$	13.31	$C^2C^1H^3$	108.04	$H^9C^7C^1H^3$	173.23
$C^2C^1H^3$	118.21	$H^{10}C^7C^1H^3$	−166.69	$C^1C^2O^4$	99.01	$H^9C^7C^1O^8$	−69.38
$C^1C^2O^4$	83.54			$C^1C^2H^5$	107.94	$H^{10}C^7C^1C^2$	−145.65
$C^1C^2H^5$	116.57			$O^4C^2H^5$	115.61	$H^{10}C^7C^1H^3$	−33.25
$O^4C^2H^5$	116.97			$C^1C^2H^6$	113.66	$H^{10}C^7C^1O^8$	84.14
$C^1C^2H^6$	113.76			$O^4C^2H^6$	113.74		
$O^4C^2H^6$	117.30			$H^5C^2H^6$	106.82		
$H^5C^2H^6$	107.51			$C^2C^1C^7$	95.13		
$H^3C^1C^7$	118.21			$H^3C^1C^7$	114.17		
$C^1C^7O^8$	83.54			$C^2C^1O^8$	130.16		
$C^1C^7H^9$	116.57			$H^3C^1O^8$	115.44		
$O^8C^7H^9$	116.96			$C^7C^1O^8$	88.59		
$C^1C^7H^{10}$	113.76			$C^1C^7H^9$	115.88		
$O^8C^7H^{10}$	117.30			$C^1C^7H^{10}$	122.86		
$H^9C^7H^{10}$	107.51			$H^9C^7H^{10}$	116.12		

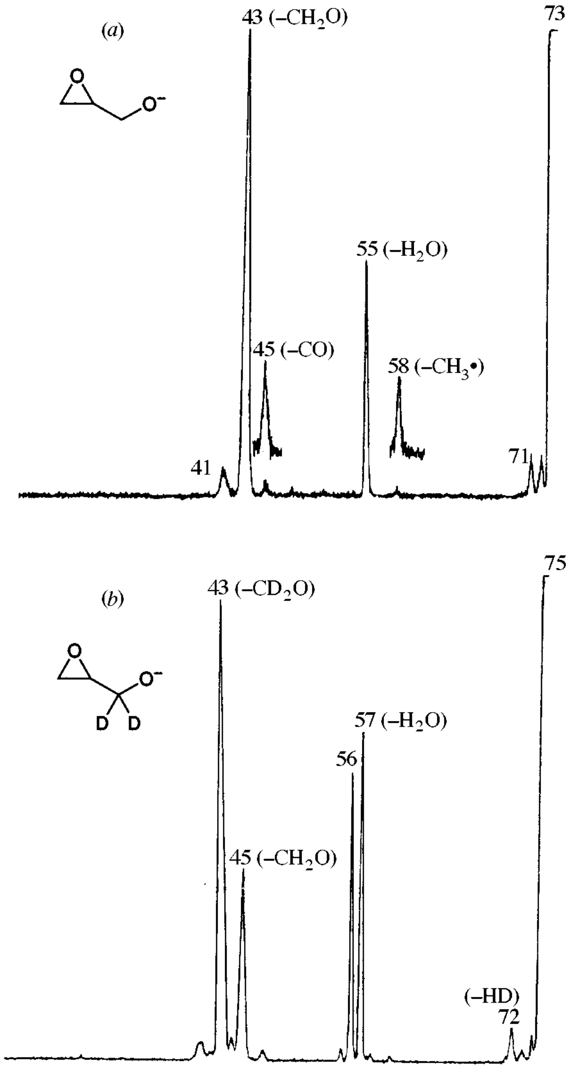

Fig. 2 The collisional activation mass spectra (MS–MS) of (*a*) the 2,3-epoxypropoxide anion, and (*b*) 2,3-epoxy[1,1-$^{2}H_2$]propoxide anion. VG ZAB 2HF instrument. For experimental details see Experimental section. The peak widths [at half height (an average of ten measurements)] for peaks in (*a*) are (volts ±0.2): *m*/*z* 55 (28.5), 45 (47.9) and 43 (40.0).

barrier should ensure that this rearrangement should be facile. The intimate mechanism of the Payne rearrangement is of interest: as the alkoxide anion approaches the epoxide ring, the adjacent ring C–O bond lengthens, inducing carbocation character at the receptor centre, *i.e.* the intramolecular nucleophilic substitution has S_N1 character.

The barrier for conversion of **A** to **B** is 122 kJ mol^{-1} and **B** is more negative in energy than **A** by 27 kJ mol^{-1}. The barriers for the two forward reactions shown in Fig. 1 are modest. Provided that the probabilities of both cyclisations are of a similar order, the calculations predict that a suitable energised 2,3-epoxypropoxide anion (**A**) should preferentially undergo the degenerate Payne rearrangement, with the possibility of a competing cyclisation to form the stable oxetane anion **B**.

We now wish to determine whether the prediction outlined above (and summarised in Scheme 1) can be confirmed experimentally.

The first task was to synthesise both **A** and **B** in the ion source of the ZAB 2HF mass spectrometer. This was done as follows. (*a*) The 2,3-epoxypropoxide anion (**A**) is the exclusive product obtained from the reaction between 2,3-epoxypropanol and HO$^-$. This was established by allowing 2,3-epoxypropan-[^{2}H]ol to react with DO$^-$ in the ion source of the ZAB mass spectrometer. The only parent ion formed was an (M − D)$^-$ species; thus deprotonation occurs exclusively at the OH site (of the unlabelled molecule) to form the required alkoxide anion. (*b*) Anion **B** can be made by two methods. The first involves deprotonation of 3-hydroxyoxetane using HO$^-$ in the ion source. This process does form the required anion in low yield but the reaction is accompanied by major polymerisation. The method of choice involves the S_N2 reaction between 3-methoxyoxetane and HO$^-$ which produces an abundant peak corresponding to the required anion **B** together with elimination of neutral methanol. The mass spectra of **B** formed by the two methods are identical.

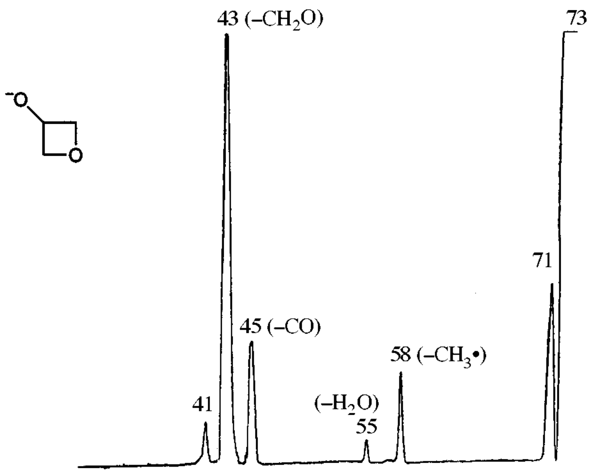

Fig. 3 The collisional activation mass spectrum (MS–MS) of oxetane anion **B**. VG ZAB 2HF instrument. The peak widths [at half height (an average of ten measurements)] for peaks in **B** (volts ±0.2) are: *m*/*z* 55 (26.0), 45 (48.2) and 43 (35.3). [The collision activation mass spectrum of the analogous [$^{2}H_2$]oxetane anion (formed by the S_N2 displacement reaction between HO$^-$ and 3-methoxy[2,2-$^{2}H_2$]oxetane) is as follows (only peaks of abundance >5% are listed): 73(H_2)20, 72(HD)75, 47(CO)35, 45(CH_2O)8, 44(CHDO)100, 43(CD_2O)32 and 41(HC_2-O^-)22].

The collision induced tandem mass spectra (MS–MS) of **A** and **B** are recorded in Figs. 2(*a*) and 3 respectively, while that of deprotonated 2,3-epoxy[1,1-$^{2}H_2$]propanol is shown in Fig. 2(*b*). The major fragmentations observed in the spectrum of **A** involve the losses of water and formaldehyde to form *m*/*z* 55 and 43, respectively. Product ion studies (Table 2) identify *m*/*z* 55 and 43 as deprotonated acrolein and the acetaldehyde enolate anion.[6]

The analogous processes in the spectrum [Fig. 2(*b*)] of the D_2 derivative are the losses of H_2O and HOD (10:8.6) together with CH_2O and CD_2O (2:5). The loss of CH_2O from the D_2 derivative can only be interpreted in terms of the operation of a cyclisation process preceding rearrangement; let us assume (in the first instance) that this is the Payne rearrangement. The observed ratio for the CH_2O and CD_2O losses (*viz.* 2:5), means that 40% of formaldehyde loss is due to simple cleavage of **A** before any cyclisation occurs. This must mean that the rates of formaldehyde loss and cyclisation are of the same order under the reaction conditions. In contrast, the ratio of losses of H_2O and HOD (10:8.6) suggests that these losses occur following ‘equilibration’ of the CH_2 and CD_2 groups, with a small deuterium isotope effect (H/D = 1.16) accompanying the process. The expected fragmentations which should follow Payne equilibration are shown (for the D_2 example) in Scheme 2. Thus fragmentation occurs both before and following rearrangement of **A**, but whether the rearrangement involves (*i*) the Payne process, (*ii*) the formation of **B**, (*iii*) an equilibrium involving **A** and **B**, or (*iv*) some combination of the above, is not known at this stage.

Consider now the spectra of **A** and **B**, which are shown in Figs. 2(*a*) and 3. Both spectra show the formation of major *m*/*z* 43 species, and product ion studies (Table 2) confirm that these correspond to the acetaldehyde enolate anion in both spectra.

Table 2 Collisional activation and charge reversal spectra of product ions[a]

Precursor ion	Product ion	Spectrum type	Spectrum CA [*m*/*z* (loss)abundance] CR [*m*/*z* (abundance)]
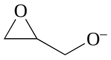 *m*/*z* 73	*m*/*z* 55 ($-H_2O$)	CR[b]	54(38), 52(72), 52(8), 40(12), 39(38), 38(36), 37(29), 36(10), 29(100), 28(30), 27(30), 26(65), 25(25)
$CH_2{=}C{=}CHO^-$[c] *m*/*z* 55		CR	54(36), 53(76), 52(10), 41(4), 40(15), 39(40), 38(42), 37(32), 36(10), 29(100), 28(34), 27(34), 26(70), 25(25), 24(5), 13(5)
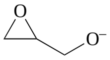	*m*/*z* 43 ($-CH_2O$)	CA CR	$41(H_2)100$ 42(100), 41(31), 40(4), 29(66), 28(23), 27(12), 26(10), 25(50), 15(3), 14(2)
$(CH_2CHO)^-$[d] *m*/*z* 43		CA CR	$41(H_2)100$ 42(100), 41(30), 40(5), 29(65), 28(26), 27(12), 26(10), 25(4), 14(2)
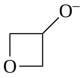 *m*/*z* 73	*m*/*z* 58 ($-CH_3^{\bullet}$)	CR	56(45), 41(38), 29(100), 28(35)
$(CHOCHO)^{\bullet -}$ *m*/*z* 58		CR	56(42), 41(34), 29(100), 28(38)
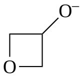	*m*/*z* 43 ($-CH_2O$)	CA CR	$41(H_2)100$ 42(100), 41(28), 40(5), 29(64), 28(25), 27(12), 26(10), 25(4), 15(4), 14(2)

[a] For details of the procedures for measuring CA and charge reversal (CR, positive ion) MS–MS data for negative ions, see Experimental section. [b] Weak spectrum—peak of abundance <5% of the base peak, is lost in baseline noise. [c] Formed by deprotonation of acrolein. [d] Formed by deprotonation of acetaldehyde.[6]

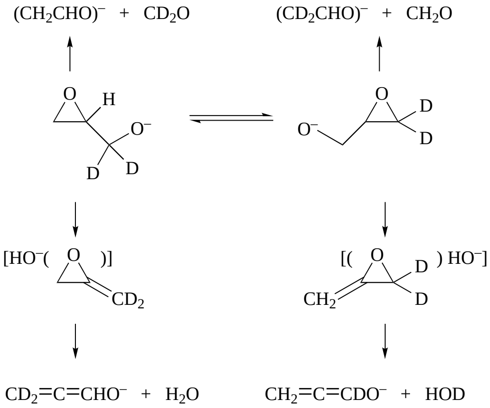

Scheme 2

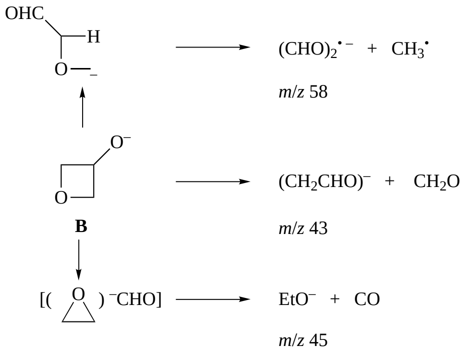

Scheme 3

However the widths at half height of the two *m*/*z* 43 peaks in the spectra are significantly different [see legends to Figs. 2(*a*) and 3], suggesting that either the mechanisms of formation of product ions, and/or the energetics of their formations are different.[7] There are two other major peaks in the spectrum of **B** which are present in trace abundances in the spectrum of **A**. These peaks *m*/*z* 58 and 45, have peak widths which are the same (within experimental error) in the spectra of both **A** and **B**. Product ion studies (Table 2) of source formed *m*/*z* 58 (from **B**) identify this ion as the succindialdehyde radical anion (*m*/*z* 58). The ion *m*/*z* 45 must be either the formate or the ethoxide anion [the ion $MeOCH_2^-$ is not a possibility since it is unstable with respect to its radical (the electron affinity[8] of $MeOCH_2^{\bullet}$ is -1.7 kJ mol^{-1})]. The species *m*/*z* 45 is not formed in the ion source so we were unable to carry out a product ion study with the VG ZAB 2HF instrument. In order to identify *m*/*z* 45, we synthesised 3-methoxy[2,2-$^2H_2$]oxetane, and the spectrum of the alkoxide anion formed from the reaction between this labelled species and HO^-, shows a peak at *m*/*z* 47 (see legend to Fig. 3) supporting the formulation of *m*/*z* 45 (from **B**) as the ethoxide anion. Fragmentations of **B** are rationalised in Scheme 3 as follows. (*i*) Loss of CH_2O occurs *via* retro-cleavage of the oxetane ring system to yield the acetaldehyde enolate anion (*m*/*z* 43). (*ii*) Ring cleavage followed by proton transfer and loss of a methyl radical gives the succinaldehyde radical anion (*m*/*z* 58). (*iii*) Partial ring cleavage followed by cyclisation gives an ethylene oxide–formyl anion ion complex, in which hydride transfer yields the ethoxide anion (*m*/*z* 45) together with carbon monoxide.

Since the peaks at *m*/*z* 58 and 45 in the spectrum of **A** have the same peak widths as the corresponding peaks in the spectrum of **B**, it can be concluded that there are some **B** fragmentations observed in the spectrum of **A**. It could be argued that because the abundances of *m*/*z* 45 and 58 in the spectrum of **A** are so small, the Payne rearrangement is operating almost to the exclusion of conversion **A** to **B**. There is however, another scenario which must also be considered. This is that **B** is formed in substantial amounts from **A**, but that the reformation of **A** and **B** occurs in preference to fragmentation of **B** (see Scheme 3) in this system. The next task is to differentiate between these two possibilities.

In order to test whether the interconversion of **A** and **B** competes with the Payne rearrangement (see Scheme 1) we need to study the fragmentations of a doubly labelled (D, ^{18}O) system. The scenario to be tested is that shown in Scheme 4. Thus we prepared the (D_2, ^{18}O) labelled 2,3-epoxypropoxide **C** (Scheme 4), and the various losses of labelled and unlabelled formaldehyde from this system will resolve the issue. We know from the

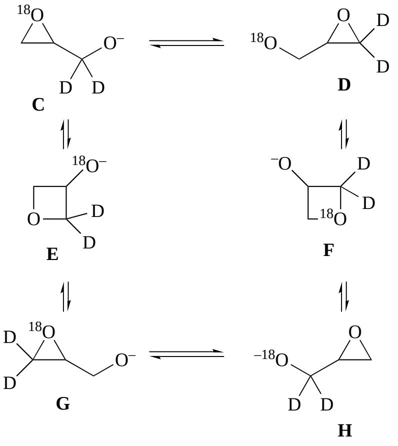

Scheme 4

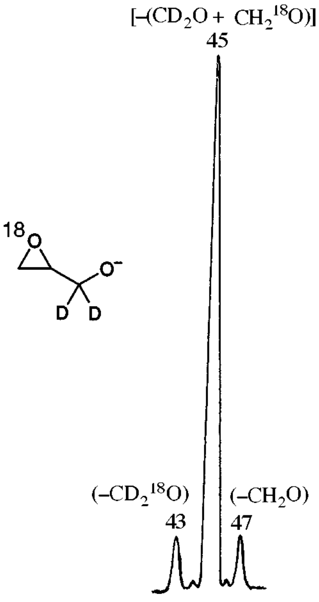

Fig. 4 Partial MS–MS data for the 2,3-[^{18}O]epoxy[1,1-$^{2}H_2$]propoxide anion. VG ZAB 2HF instrument.

spectrum of the D_2 labelled ion [Fig. 2(*b*)] that 60% of the loss of formaldehyde occurs following cyclisation process(es). If cyclisation involves only the Payne rearrangement, the spectrum of **C** will show only fragmentations of **C** and **D** [loss of CD_2O and $CH_2{}^{18}O$ (32 Da): see Scheme 4 and *cf.* Scheme 2]. If oxetane ions **E** and **F** are involved, losses of CH_2O (30 Da), CD_2O and $CH_2{}^{18}O$ (32) and $CD_2{}^{18}O$ (34) will occur by retro-processes of the oxetanes **E** and **H**, and/or from **C**, **D**, **G** and **H** (*cf.* Scheme 2). The spectrum of **C** (Fig. 4) shows losses of 30, 32 and 34 in the ratio 11 : 100 : 11. This means that of the CH_2O loss which follows cyclisation, *ca.* 40% occurs following Payne equilibration only, while *ca.* 60% involves both Payne and oxetane equilibration prior to fragmentation. No other mechanistic interpretation can account for the losses of CH_2O and $CD_2{}^{18}O$ in this system.

The experimental data confirm the scenario outlined in Scheme 1 and Fig. 1. The 2,3-epoxypropoxide anion (**A**), on collisional activation in the gas phase, (*i*) undergoes the degenerate Payne rearrangement together with competitive conversion of **A** to **B**, with the Payne rearrangement being the more facile of the two, and (*ii*) loses CH_2O from energised **A**. The latter process occurs principally by the simple cleavage–ring opening process shown in Scheme 2 (even though **A** and **B** undergo substantial equilibration, fragmentation products from **B** are of minor abundance in the spectrum of **A**). The losses of CH_2O occur as follows: 40% before Payne rearrangement, 25% after Payne rearrangement but before conversion to **B**, and 35% following equilibration of **A** and **B**.

Let us now consider the energetics of the interconversion of **A** to **B** in comparison to those of fragmentations of **A** and **B**. We have not carried out *ab initio* calculations on the cleavage reactions, but we have calculated the thermochemistry of the fragmentation processes from experimentally derived data[9] (see Scheme 5). Compare first the loss of CH_2O from **A** and the Payne rearrangement of **A**. Although the cleavage process is favourable thermodynamically [$\Delta H = -90$ kJ mol^{-1} (Scheme 5)], the relative extents of rearrangement and cleavage will be controlled by the rates of the two reactions. The Payne rearrangement has a low barrier to the transition state [45 kJ mol^{-1} (Fig. 1)], but the reaction channel will be narrow leading to a modest frequency factor (or Arrhenius **A** factor).[5] In contrast, the simple cleavage will have a higher barrier to the transition state, but this should be counteracted by the favourable **A** factor of the cleavage reaction. Thus it is not unreasonable that the rates of loss of CH_2O from **A** and Payne rearrangement of **A** should be of the same order.

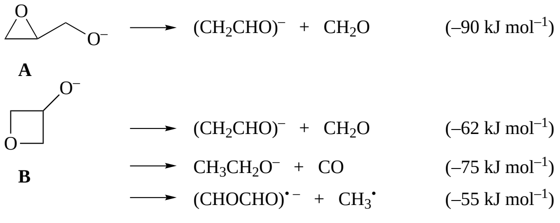

Scheme 5

The final question to be resolved is why the conversion of **B** to **A** is more facile than fragmentation of **B** in the equilibrating **A**/**B** system, in spite of the fact that the cleavage processes (of **B**) are exothermic (Scheme 5). This is an unusual situation. The answer must be that under the reaction conditions, **B** is formed with enough excess energy to reform **A**, but not sufficient to effect major fragmentation of **B**. This seems reasonable for those cleavage of **B** which involve the losses of CO and $CH_3{}^{\bullet}$, since both reactions are complex, multistep and should be inefficient (see Scheme 3). In contrast, the loss of CH_2O from **B** to form $(CH_2CHO)^-$ should be facile if it is a simple retro-process (see Scheme 3). However it is known that retro-cleavage of an oxetane in solution is an unfavourable reaction, requiring temperatures in excess of 400 °C:[11] perhaps the gas phase reaction is also a high energy process. The fragmentation data of the $(M - H)^-$ ion of the D_2 oxetane derivative supports this proposal. If the D_2 parent anion were to undergo simple retro-processes, losses of CH_2O and CD_2O should be observed (in the ratio 1 : 1 if the secondary deuterium kinetic isotope effect is 1.0). However, the spectrum (see legend to Fig. 3) shows losses of CH_2O, CHDO and CH_2O (32 : 100 : 8), indicating that the reaction cannot be a simple retro-process, since H/D rearrangement (together with the operation of a significant deuterium kinetic isotope effect) precedes cleavage. The overall process is inefficient; a mechanistic rationale is shown in Scheme 6 where it is suggested that carbanion formation on the ring is a prerequisite to cleavage, and that these processes are accompanied by cross ring H/D scrambling. The ratio of losses of the variously deuterated formaldehydes indicates that process **a** must be strongly favoured over process **b**, even though it is not possible to calculate k_H/k_D for individual steps from available data.

In conclusion, energised 2,3-epoxypropoxide anions undergo the degenerate Payne rearrangement in the gas phase *via* a three-centre mechanism. This rearrangement competes with the alternative cyclisation *via* a four-membered transition state to form an oxetane alkoxide species.

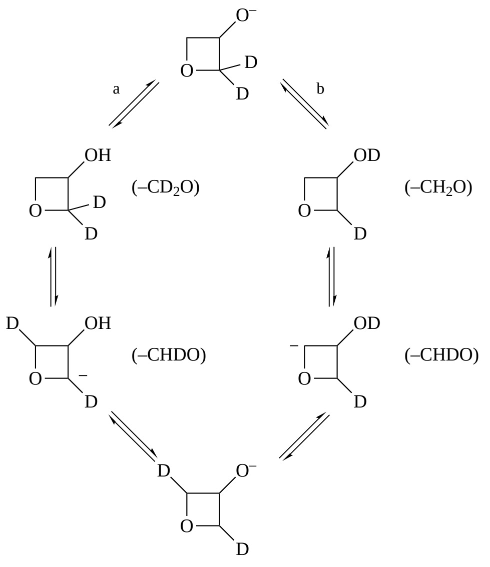

Scheme 6

Experimental

Mass spectrometric methods

Collisional activation (CA) mass spectra (MS–MS) were determined with a VG ZAB 2HF mass spectrometer.[12] Full operating details have been reported.[13] Specific details were as follows: the chemical ionisation slit was used in the chemical ionisation source, the ionising energy was 70 eV, the ion source temperature was 100 °C, and the accelerating voltage was 7 kV. The liquid samples were introduced through the septum inlet with no heating [measured pressure of sample 1×10^{-6} Torr (1 Torr = 133.322 Pa)]. Deprotonation was effected using HO^- (from H_2O: measured pressure 1×10^{-5} Torr). The estimated source pressure was 10^{-1} Torr. Argon was used in the second collision cell (measured pressure, outside the cell, 2×10^{-7} Torr), giving a 10% reduction in the main beam, equivalent to single collision conditions. CID MS–MS measurements involved using the magnet to choose the ion under study [normally the $(M - H)^-$ species], collision activating it (see above), and scanning the electric sector to analyse the resultant product anions. Charge reversal (CR) (positive ion) MS–MS data for negative ions were obtained as for CA MS–MS data, except that the electric sector potential was reversed to allow the transmission of positively charged product ions (for full details see ref. 14).

Ab initio calculations

The GAUSSIAN 94[4] suite of programs was used for all calculations. The computational platforms used were a Silicon Graphics Indigo²xZ workstation and a Silicon Graphics Power Challenge. The geometrics of the local minima and the transition states were optimised at the RHF/6-31g(d) level of theory. Harmonic frequency analyses were performed on each stationary point in order to characterise them as either a local minimum or transition state. A local minimum is characterised by possessing all real vibrationary frequencies and its Hessian matrix possessing all positive eigenvalues. A transition state is characterised by possessing one (and only one) imaginary frequency and its Hessian matrix possessing one (and only one) negative eigenvalue. Intrinsic reaction coordinate (IRC) calculations were performed (beginning from both transition structures) to verify that each transition structure connected particular local minima.

The energy of each structure at 0 K was calculated using both G2[15] and G2(MP2)[16] theories. Both theoretical schemes aim to approximate a QCISD(T)/6-311+g(3df,2p) single point energy at an MP2(full)/6-31g(d) optimised geometry. Both the G2(0 K) and G2(MP2)(0 K) energies include a scaled (0.8929)[15] zero point vibrational energy correction based on the rhf/6-31g(d) optimised geometry.

Unlabelled compounds

Acetaldehyde, acrolein, 2,3-epoxypropanol, ethanol and succindialdehyde were commercial samples. 3-Hydroxyoxetane[17] and 3-methoxyoxetane[18] were prepared by reported procedures.

Labelled compounds

These were synthesised as outlined below. The purity of all products was established ^1H NMR and positive ion mass spectrometry. The extent of incorporation (of D and/or ^{18}O) was established by either positive or negative ion mass spectrometry.

2,3-Epoxypropan[^2H]ol was prepared by exchange of the appropriate alcohol with D_2O, until the D_1 incorporation was >95% as shown by positive ion mass spectrometry.

2,3-Epoxy[1,1-$^2H_2$]propanol. A mixture of lithium aluminium deuteride (2.5 g) in anhydrous diethyl ether (75 cm^3) was cooled to 0 °C and a solution of acrylyl chloride (5 g) in diethyl ether (25 cm^3) added at such a rate that the temperature remained below 5 °C. The mixture was then stirred at 20 °C for 2 h, cooled to 0 °C, and aqueous sodium hydroxide (15%, 20 cm^3) was added. The mixture was filtered, the filtrate washed with diethyl ether (10 cm^3), the combined organic layers dried (Na_2SO_4), the solvent removed *in vacuo*, and the residue distilled to yield [1,1-$^2H_2$]allyl alcohol (1.4 g, 42% yield, D_2 > 99%).

A solution of *meta*-chloroperbenzoic acid (4 g) in anhydrous methylene chloride (25 cm^3) was added, at 0 °C, to a solution of [1,1-$^2H_2$]allyl alcohol (1.0 g) in methylene chloride (50 cm^3). The mixture was stirred at 20 °C for 20 h, filtered, the remaining solution was shaken with aqueous sodium hydroxide (4 M) until the aqueous phase remained alkaline, then water until the aqueous phase was neutral. The organic phase was dried ($MgSO_4$), concentrated *in vacuo*, and distilled to yield 2,3-epoxy[1,1-$^2H_2$]propanol (0.5 g, 47% yield, D_2 = 99%).

2,3-[^{18}O]Epoxy[1,1-$^2H_2$]propanol. This was prepared from [1,2-$^2H_2$]allyl alcohol (see above) using the $Ag_2O/I_2/H_2{}^{18}O$ (^{18}O = 96%) method.[19] Yield 53%, D_2 = 99%, ^{18}O = 80% (this method is known to result in some loss of ^{18}O: no explanation for this was given;[19] however, the only source of ^{16}O is the Ag_2O).

3-Methoxy[2,2-$^2H_2$]oxetane. [1,1-$^2H_2$]Allyl alcohol (1.1 g) was dissolved in anhydrous methanol (30 cm^3) containing concentrated sulfuric acid (2 drops). *N*-Bromosuccinimide (3.25 g) was added in small portions and the mixture stirred at 20 °C for 3 h. The solvent was removed *in vacuo*, water (50 cm^3) was added, the mixture extracted with diethyl ether (3×10 cm^3), the organic layer dried ($MgSO_4$), concentrated, distilled to yield 3-bromo-2-methoxy[1,1-$^2H_2$]propanol (1.4 g), which was cyclised (using NaH in anhydrous diethyl ether)[18] to yield 3-methoxy[2,2-$^2H_2$]oxetane (0.7 g, D_2 = 99%).

Acknowledgements

We thank the Australian Research Council for funding our negative ion programme. One of us (S. D.) thanks the ARC for a research associate position.

References

1 G. B. Payne, *J. Am. Chem. Soc.*, 1962, **27**, 3819.
2 C. H. Behrens, S. Y. Ko, B. Sharpless and F. J. Walker, *J. Org. Chem.*, 1985, **50**, 5687.
3 C. Bonini, C. Guikiano, R. Righi and L. Rossi, *Tetrahedron Lett.*, 1992, 7429.
4 GAUSSIAN94, Revision C3, M. J. Frish, G. W. Trucks, H. B. Schlegel, P. M. W. Gill, B. G. Johnson, M. A. Robb, J. R. Cheeseman, T. Keith, G. A. Petersson, J. A. Montgomery, K. Raghavachari, M. A. Al-Latham, V. H. Zakrzewski, J. V. Ortiz, J. B. Foresman, J. Cioslowski, B. B. Stefanov, A. Nanayakkara,

M. Challacombe, C. Y. Peng, P. V. Ayala, W. Chen, M. W. Wong, J. L. Andres, E. S. Replogle, R. Gomperts, R. L. Martin, D. J. Fox, J. S. Binkley, D. J. Defrees, J. Baker, J. P. Stewart, M. Head-Gordon, C. Gonzalez and J. A. Pople, Gaussian Inc., Pittsburgh, PA, 1995.

5 S. Okada, Y. Abe, S. Tanaguchi and S. Yamabe, *J. Am. Chem. Soc.*, 1987, **109**, 295.

6 K. M. Downard, J. C. Sheldon and J. H. Bowie, *Int. J. Mass Spectrom. Ion. Proc.*, 1988, **86**, 217.

7 R. G. Cooks, J. H. Beynon, R. M. Caprioli and G. R. Lester, *Metastable Ions*, Elsevier, New York, 1973, pp. 57–70.

8 C. H. DePuy, V. M. Bierbaum and R. Damrauer, *J. Am. Chem. Soc.*, 1984, **106**, 4051.

9 J. W. Benson, *Thermochemical Kinetics*, Wiley, New York, 1967; S. G. Lias, J. E. Bartmess, J. F. Liebman, J. L. Holmes, R. D. Levin and W. G. Mallard, *Gas Phase Ion and Thermal Thermochemistry*, *J. Phys. Chem. Ref. Data 17*, 1988, Suppl. 1 (Computer version); G. Aylward and T. Findlay, *S.I. Chemical Data*, Wiley, Brisbane, New York, 3rd ed., 1994; M. J. Travers and G. B. Ellison, *Experimentally Derived Electron Affinities to 1989*, Department of Chemistry and Biochemistry, University of Colorado at Boulder.

10 M. J. S. Dewar, E. G. Zoeblish and E. F. Healy, *J. Am. Chem. Soc.*, 1985, **107**, 3902.

11 M. J. Clarke and K. A. Holbrook, *J. Chem. Soc., Faraday Trans. 1*, 1977, **73**, 890.

12 VG ZAB 2HF, VG Analytical, Manchester, UK.

13 M. B. Stringer, J. L. Holmes and J. H. Bowie, *J. Am. Chem. Soc.*, 1986, **108**, 3888.

14 J. H. Bowie and T. Blumenthal, *J. Am. Chem. Soc.*, 1995, **97**, 2959; I. Howe, J. H. Bowie, J. E. Szulejko and J. H. Beynon, *Int. J. Mass Spectrom. Ion. Phys.*, 1980, **34**, 99.

15 L. A. Curtiss, K. Raghavachari, G. W. Trucks and J. A. Pople, *J. Chem. Phys.*, 1991, **94**, 7221.

16 L. A. Curtiss, K. Raghavachari and J. A. Pople, *J. Chem. Phys.*, 1993, **98**, 1293.

17 K. Baum, P. T. Berkowitz, V. Grakanskas and T. G. Archibald, *J. Org. Chem.*, 1983, **48**, 2953.

18 J. A. Wojtowicz, R. J. Polak and J. A. Zaslowsky, *J. Org. Chem.*, 1971, **36**, 2232.

19 B. Borhan, S. Nazarian, E. M. Stocking, B. D. Hammock and M. J. Kurth, *J. Org. Chem.*, 1994, **59**, 4316.

Paper 7/01965C
Received 20*th March* 1997
Accepted 12*th May* 1997